ELSEVIER

Solution conformation of phakellistatin 8 investigated by molecular dynamics simulations

Oxana Galzitskaya* and Amedeo Caflisch†

**Institute of Protein Research, Russian Academy of Sciences, Pushchino, Moscow Region, Russian Federation*
†Department of Biochemistry, University of Zurich, Zurich, Switzerland

Phakellistatin 8 is a cyclic decapeptide that inhibits cancer cell growth and has sequence and structure similar to antamanide. In molecular dynamics simulations of phakellistatin 8 in water, the decapeptide ring undergoes a conformational change from the saddle-like crystal structure to a more elongated conformation by a transition of the Tyr9 main chain from the α_L to an extended structure. This is coupled to the loss of the NH9–O6 β-turn hydrogen bond and the transient dissociation of the Pro7–Tyr9 side-chain packing. Furthermore, the water molecule acting as a transannular bridge forms an additional hydrogen bond with phakellistatin 8, namely with the NH group of Val5 besides those already present in the crystal structure, i.e., with the NH of Ile10 and the CO of Leu6. The α-turn hydrogen bond between the Phe4 amide hydrogen and the Ile10 carbonyl oxygen is always present. The solution conformations of the two cyclic decapeptides are similar, in particular in the region involving the NH4–O10 α turn of phakellistatin 8 and the NH5–O1 α turn of antamanide. The simulation results suggest that in aqueous solution the conformation of phakellistatin 8 is more extended than in the crystalline state, and on a nanosecond time scale phakellistatin 8 is more flexible than antamanide. © 1999 by Elsevier Science Inc.

Keywords: phakellistatin 8, antamanide, cyclic peptide, molecular dynamics, anticancer agent

1. INTRODUCTION

The isolation of three cyclic decapeptides, phakellistatins 7, 8, and 9, from the marine sponge *Phakellia costata* has been reported.[1] Phakellistatins 7–9 are the first cancer cell growth-inhibitory cyclic decapeptides. For this reason the X-ray crystallographic structure of phakellistatin 8, cyclo[Pro1–Pro2–Ile3–Phe4–Val5–Leu6–Pro7–Pro8–Tyr9–Ile10], has been determined.[2] The three peptides are closely related, the only differences from phakellistatin 8 being Val5Ala in phakellistatin 7, and Ile10Val in phakellistatin 9.

It is known that the knowledge of the crystal structure of a molecule is sometimes insufficient for understanding its biological properties, which are intimately connected to the molecular flexibility. Moreover, both average structure and mobility are affected by the presence of solvent molecules. Hence, this work is concerned with the molecular dynamics investigation of the solution conformation and dynamic behavior of phakellistatin 8 (the suffix 8 is dropped henceforth) and the comparison with the cyclic decapeptide antamanide (cyclo[Val1–Pro2–Pro3–Ala4–Phe5–Phe6–Pro7–Pro8–Phe9–Phe10], name derived from the term *antiamanita peptide*), which is a component of the poisonous mushroom *Amanita phalloides*. Phakellistatin and antamanide are relatively similar in amino acid composition, overall backbone structure, proline ring conformations, and the presence of nearly identical α turns involving one of the two Pro–Pro pairs.[2]

While there are few studies of phakellistatin, antamanide is one of the most extensively examined cyclic peptides. Its structural characteristics were first investigated by X-ray crystallography[3] and the solution conformation and motional freedom have been studied by NMR spectroscopy[4,5] and molecular dynamics simulations at room temperature[6–9] and more recently at a temperature of 400 K.[10] All of the aforementioned simulation studies were performed without explicit solvent molecules except for an 800-ps molecular dynamics run of antamanide in chloroform[7] and a 1.4-ns simulation of antamanide and eight water molecules in chloroform at 250 K (first 1.0 ns) and 290 K (from 1.0 to 1.4 ns).[11] To the best of our knowledge the present study contains the first molecular dynamics simulation of antamanide in aqueous solution (explicit water molecules) and the first computational study of phakellistatin. The present simulations yield structural information that can be compared with the available experimental data and provide a model of (one of) the preferred solution conforma-

Address reprint requets to: Amedeo Caflisch, Department of Biochemistry, University of Zürich, Winterthurerstrasse 190, CH-8057 Zürich, Switzerland. Tel.: (41 1) 635 55 21; E-mail: caflisch@bioc.unizh.ch

655 Avenue of the Americas, New York, NY 10010
1093-3263/99/$–see front matter
PIIS1093-3263(99)00017-0

tion(s) of phakellistatin and its dynamic behavior on a nanosecond time scale.

2. METHODS

All simulations were carried out with the CHARMM program,[12] using the polar hydrogen parameter set (param19), i.e., aliphatic and aromatic hydrogen atoms are considered as part of the carbon atoms to which they are covalently bound. The cutoff for the nonbonded interactions was the default value of 7.5 Å[13] and the TIP3P model was employed for the water molecules.[14]

The coordinates of the heavy atoms of phakellistatin and antamanide were kindly provided by D.L. Herald.[2] Coordinates for polar hydrogen atoms were built with the HBUILD algorithm in CHARMM.[15] The structure of phakellistatin was then translated as a rigid body into a sphere of preequilibrated water molecules of 21-Å radius. Water molecules whose oxygen coordinates were within 2.8 Å of any heavy atom of the peptide were removed. This was followed by a 1-ps equilibration of the water molecules around the rigid solute. The solute and equilibrated solvent were then rotated and reimmersed in the original water sphere. Overlapping water molecules were deleted and the solvent was again equilibrated around the rigid solute. Reimmersion and equilibration were performed three times to fill small cavities with solvent molecules. The system after the fourth immersion consisted of 89 phakellistatin atoms and 1 270 water molecules, for a total of 3 899 atoms. A similar protocol was used for antamanide, yielding 90 atoms for the solute and 1 261 water molecules for a total of 3 873 atoms.

The solution behavior of the cyclic decapeptides was investigated by calculating three trajectories for phakellistatin and two for antamanide. All trajectories were started from the final frame obtained at the end of the water equilibration around the rigid solute. Two different restraining potentials were used to prevent the solute from leaving the central region of the sphere. In one simulation (called AnC henceforth) the center of mass of antamanide was constrained at the center of the water sphere by a harmonic potential with force constant of 50 kcal/(mol Å^2).[16] In a second simulation (called AnA henceforth) the antamanide atom closest to the center of the water sphere was constrained by a harmonic potential with force constant of 100 kcal/(mol Å^2). Each trajectory consisted of a 40-ps equilibration with rescaling of the velocities every 20 steps at a temperature of 300 K followed by 2.5-ns production dynamics without any reassignment of the velocities. The same equilibration protocol and restraining potentials were used for phakellistatin. In addition, the simulation with constraint on the center of mass was branched at the beginning of the production run by random reassignment of the velocities from a Gaussian distribution. The phakellistatin runs will be referred as PhC1, PhC2, and PhA. Two different potentials were used to evaluate the effects of the restraints. These appear to be negligible since the differences between the PhC1 and PhA runs are comparable to the differences between the PhC1 and PhC2 runs.

The atoms in the spherical region of 17-Å radius were treated by Newtonian dynamics, whereas the solvent molecules in the spherical shell from 17 to 21 Å were treated by Langevin dynamics with a deformable boundary potential.[17] Bond lengths to hydrogen atoms were constrained by the SHAKE algorithm.[18] The leap-frog integrator was used in all runs with an integration step of 2 fs and the nonbonding pair list was updated every 10 steps. Coordinate frames were saved every 0.5 ps for a total of 5 000 conformations for each trajectory.

3. RESULTS

First, the overall behavior along the trajectories of phakellistatin is analyzed and compared with the antamanide runs. Particular attention is given to the deviation from the crystal structure, the changes in the backbone conformation and intramolecular hydrogen bonds, and the motion of the side chains of the aromatic and proline residues. Finally, a prediction is made for the preferred conformation of phakellistatin in water and its dynamic behavior on a nanosecond time scale.

3.1. Global behavior

The C_α and heavy-atom root mean square deviation (RMSD) from the X-ray structure as a function of time are given in Figure 1 for the PhC1 and AnC trajectories. In the phakellistatin simulations a relatively large conformational change takes place after about 1.2 ns (PhC1 run; Figure 1a), 0.2 ns (PhC2, not shown), and 0.4 ns (PhA, not shown). Most of the following analysis focuses on the final 0.5 ns of the trajectories (i.e., from 2.0 to 2.5 ns) because the conformational change of phakellistatin takes place earlier. The C_α RMSD from the crystal structure averaged over the final 0.5 ns is 1.1, 1.2, and 1.6 Å for the run PhC1, PhC2, and PhA, respectively. The corresponding values for the heavy-atom RMSD are 2.1, 2.2, and 2.6 Å. The conformation of the phakellistatin macrocycle changes from the saddle-like crystal structure[2] to a more elongated conformation (Figure 2a). This is coupled to the Tyr9 main-chain dihedral transition from the α_L to an extended conformation (Section 3.2), the loss of the NH9–O6 β-turn hydrogen bond (Section 3.3), and the transient dissociation of the Pro7–Tyr9 side-chain packing (Section 3.4).

Smaller deviations are found in the antamanide trajectories (Figures 1b and 2b). The C_α RMSD from the X-ray structure

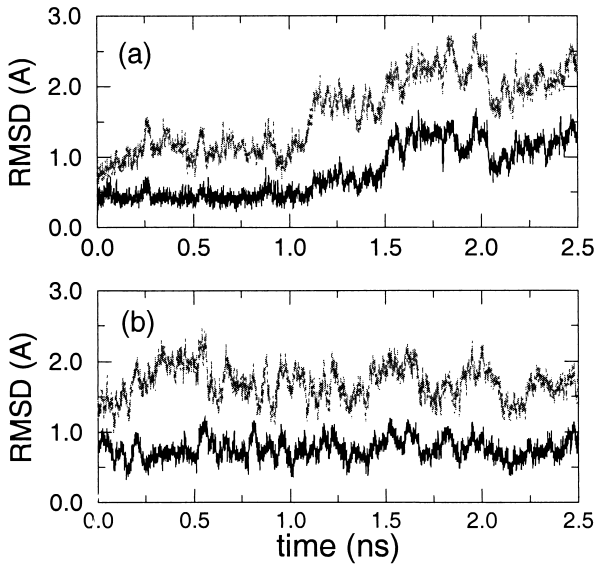

Figure 1. C_α (continuous line) and heavy-atom (dotted line) RMSD from the crystal structure as a function of time for the (a) PhC1 and (b) AnC simulations.

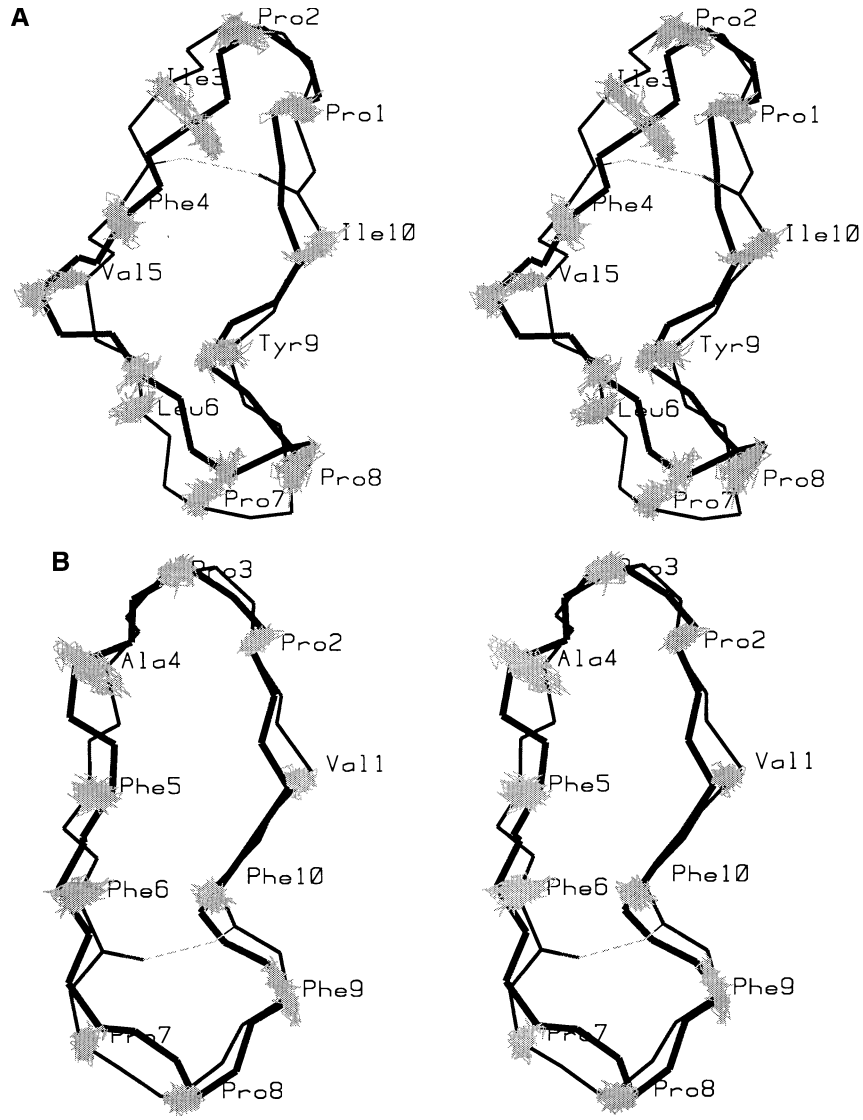

Figure 2. (a) Stereoplot (relaxed view) of the phakellistatin backbone in the crystal structure (thick line) and the conformation at the end of the PhC1 run (thin line). The trace of the C_α atoms is plotted in gray for snapshots taken every 5 ps from the PhC1 run. The α-turn hydrogen bond is drawn with a dashed line. (b) Same as in (a) for the antamanide simulation AnC.

averaged over the final 0.5 ns is 0.8 Å (AnC run; Figure 1b) and 0.7 Å (AnA, not shown), while the heavy-atom RMSD is 1.7 Å (AnC) and 1.6 Å (AnA). As a basis of comparison in a simulation of antamanide with eight water molecules in chloroform, which used a different force field, the C_α (all heavy-atom) RMSD from the X-ray structure was 0.8 Å (1.7 Å) after 1.0 ns at 250 K.[11] It is evident from Figure 2b that the antamanide macrocycle does not undergo any major conformational change. There are only minor fluctuations in the backbone of antamanide and the largest motion involves the Ala4–Phe5 amide bond. This is in agreement with the measured values of the $^{13}C_\alpha$ transverse relaxation rate constants (R_2), which are larger for the C_α of Ala4, Phe5, and Phe6 than for the remaining residues.[11]

It is interesting to note that the solution conformations of phakellistatin and antamanide are similar, in particular in the region forming the α turn (see below). After optimal superposition of the 10 C_α atoms, shifted by 1 residue for symmetry reasons (phakellistatin Pro1–Pro2 matched to antamanide Pro2–Pro3, etc.), the C_α RMSD (in Ångstroms) between the conformations saved at the end of the dynamics runs are as follows: 0.92 (PhC1–AnC), 0.95 (PhC2–AnC), 1.03 (PhA–AnC), 1.22 (PhC1–AnA), 0.91 (PhC2–AnA), and 1.26 (PhA–AnA). These values are smaller than the C_α RMSD between the X-ray structure of phakellistatin and the final conformations of AnC (1.59 Å) and AnA (1.44 Å). Hence, the conformational transition observed during dynamics yields an aqueous conformation of phakellistatin whose main-chain structure is similar to that of antamanide.

3.2. Backbone dihedral angles

In the crystal structure of both cyclic peptides two residues occupy energetically unfavorable regions of the Ramachandran map: antamanide Phe5 and Phe10 are in the α_L region,[3] while phakellistatin Tyr9 and Phe4 occupy the α_L and (70°, −40°) region, respectively.[2] Left-handed α helices are not present in linear peptides for energetic reasons, i.e., close contacts be-

tween side chain and peptide backbone. On the other hand, residues in the α_L conformation appear sporadically in cyclic peptides.[19] During the phakellistatin simulations the main-chain dihedral angles of Tyr9 change abruptly from the α_L region to an extended conformation at 1.2 ns (run PhC1; Figure 3a and b), 0.2 ns (PhC2), and 0.4 ns (PhA). This is followed by a change in the ψ angle of Phe4 from about $-60°$ to about 50° (Figure 3a and b). Table 1 contains the average values and standard deviations of the torsion angles for the final 0.5 ns of the phakellistatin runs. There are only minor differences in the average values of the main-chain dihedral angles. Moreover, the fluctuations are small, the largest ones involving the ϕ angle of Leu6 and the ψ of Pro2 and Phe4. Therefore, the three phakellistatin simulations have converged toward a common conformation that is proposed as the preferred solution structure.

In the molecular dynamics simulations the X-ray conformation of the antamanide macrocycle is more stable than that of phakellistatin. In the AnC and AnA trajectories the values of the main-chain dihedral angles were almost constant except for one rotation of the Ala4–Phe5 peptide unit from $\psi_4 = -45°$ and $\phi_5 = 60°$ to $\psi_4 = 120°$ and $\phi_5 = -80°$ after about 1.0 ns of AnC. Such a transition was previously observed at about 0.1 ns of a 0.5-ns stochastic dynamics simulation of antamanide in vacuo[8] and in a 33-ps simulation in vacuo, which used 40 NOE constraints obtained from measurements in chloroform at 253 K.[6] Table 2 contains the average values and standard deviations of the backbone dihedral angles for the final 0.5 ns of the antamanide runs. From the simulation results the main-chain conformation of antamanide is similar to that derived from NMR data in chloroform (Table 2). The main chain in the AnC simulation is close to the one extracted from the aforementioned simulation in vacuo with 40 NOE constraints,[6] while the AnA backbone dihedrals are similar to those of an optimally populated structure obtained with a stochastic search protocol that used 23 backbone–backbone distance constraints derived from cross-peak intensities in NOESY and ROESY spectra.[20] The main discrepancies between the simulation results in water and the data extracted from NMR measurements in chloroform are in the values of ψ_3 (in both AnC and AnA), the values of ψ_9 and ϕ_{10} (only in AnC), and the values of ψ_{10} and ϕ_1 (only in AnA). The preferred conformation(s) of a peptide in chloroform is not necessarily similar to the one(s) in water because a maximum of intramolecular hydrogen bonds are formed in chloroform but not in water.

Both cyclic peptides have two *cis* peptide bonds in their crystal structure. For phakellistatin these are Pro1–Pro2 ($\omega_1 = 7°$) and Pro7–Pro8 ($\omega_7 = 11°$),[2] and for antamanide Pro2–Pro3 ($\omega_2 = 2°$) and Pro7–Pro8 ($\omega_7 = 4°$).[3] The *cis* peptide bonds were stable during all dynamics simulations. The average values over the PhC1 trajectory were $-9° \pm 8°$ and $-4° \pm 8°$ for ω_1 and ω_7, respectively. For the AnC run the average values were $-5° \pm 7°$ and $-8° \pm 8°$ for ω_2 and ω_7, respectively. Similar values were found for the other trajectories.

3.3. Hydrogen bonds

Two of the three hydrogen bonds present in the crystal structure of phakellistatin are lost in all simulations (Figure 4a and b). First, the β-turn hydrogen bond between NH9 and CO6 is broken at about 1.2, 0.2, and 0.4 ns in the PhC1, PhC2, and PhA runs, respectively. This is followed by the rupture of the γ-turn hydrogen bond between NH5 and CO3 at about 1.5 ns (run PhC1), 0.2 ns (PhC2), and 0.8 ns (PhA). The disruption of the β-turn hydrogen bond is coupled to the transition of Tyr9 from the α_L to the β region of the Ramachandran map while the rupture of the γ-turn hydrogen bond is associated with the change in the ψ_4 dihedral angle (Figure 3b). The loss of intramolecular hydrogen bonds (from an average of 3.4 ± 0.8 in the first 1.5 ns of PhC1 to an average of 1.4 ± 0.6 in the last 1.0 ns) is balanced by an increase in the number of phakellistatin–water hydrogen bonds (from an average of 19 ± 2 to 22 ± 2). As a consequence, the total count of intramolecular plus phakellistatin–solvent hydrogen bonds is almost constant along the trajectories. In all simulations of phakellistatin there is a water molecule donating to the main-chain carbonyl group of Leu6 and accepting from the main-chain amide of Ile10 in agreement with the crystal structure[2] (see also Section 3.6).

For antamanide the two crystal structure α-turn hydrogen bonds are preserved in the two simulations except for the NH5–O1 bond, which comes apart after about 1.0 ns of AnC (Figure 4c and d). This is coupled to the formation of the NH6–O4 hydrogen bond in AnC, in agreement with structural data derived from NMR measurements,[6] and originates from the rotation of the peptide unit involving the backbone dihedrals ψ_4 and ϕ_5 (see Section 3.2). There is only a minor variation in the number of hydrogen bonds in antamanide (1.9 ± 0.7 and 2.3 ± 0.5 in the whole AnC and AnA run, respectively) and the number of antamanide–solvent hydrogen

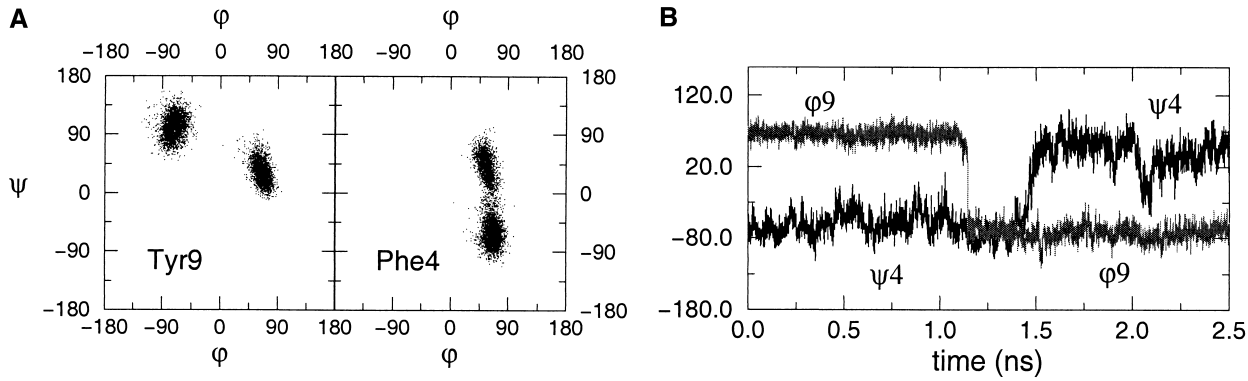

Figure 3. Backbone conformational changes in the phakellistatin run PhC1. Values are plotted in increments of 0.5 ps. (a) Ramachandran plot; (b) time series.

Table 1. Dihedral angles of phakellistatin

	Pro1	Pro2	Ile3	Phe4	Val5	Leu6	Pro7	Pro8	Tyr9	Ile10
ϕ										
x-ray[a]	−65	−90	−88	71	−101	−118	−62	−92	75	−88
PhC1	−62 (9)	−95 (10)	−69 (12)	58 (9)	−98 (14)	−88 (13)	−64 (9)	−69 (8)	−73 (11)	−86 (14)
PhC2	−62 (8)	−97 (9)	−74 (12)	60 (9)	−101 (14)	−93 (18)	−61 (10)	−71 (8)	−75 (11)	−88 (16)
PhA	−63 (9)	−84 (13)	−77 (14)	60 (10)	−95 (13)	−100 (17)	−60 (10)	−69 (8)	−72 (11)	−96 (17)
ψ										
x-ray	153	1	−45	−41	−5	146	143	20	31	153
PhC1	136 (7)	13 (18)	−54 (11)	32 (24)	−75 (13)	141 (10)	138 (7)	142 (15)	102 (17)	138 (14)
PhC2	137 (7)	22 (15)	−57 (9)	40 (22)	−79 (14)	140 (21)	137 (8)	142 (19)	105 (21)	132 (13)
PhA	148 (16)	−32 (32)	−23 (19)	75 (20)	−84 (15)	142 (19)	137 (7)	141 (24)	112 (15)	129 (12)
ω										
x-ray	7	−173	174	−161	175	179	11	167	174	167
PhC1	−10 (7)	−173 (8)	176 (8)	−178 (7)	−177 (6)	171 (8)	−6 (7)	−172 (7)	−176 (6)	170 (6)
PhC2	−11 (8)	−172 (8)	175 (7)	−179 (7)	−176 (6)	173 (8)	−5 (8)	−172 (8)	−178 (7)	171 (6)
PhA	−7 (8)	−168 (8)	177 (7)	−179 (7)	−174 (6)	174 (8)	−5 (8)	−170 (8)	−178 (7)	171 (6)
χ_1										
x-ray			176	−64	65	−73			−48	−71
PhC1			0 (54)	−70 (14)	−178 (10)	−66 (17)			−67 (12)	−52 (18)
PhC2			−54 (13)	−64 (10)	−178 (10)	−66 (67)			−66 (11)	−19 (55)
PhA			−160 (11)	−57 (11)	−159 (38)	−71 (32)			−68 (10)	−34 (41)
χ_2										
x-ray			−59	89		165			−66	165
PhC1			167 (25)	137 (86)		171 (8)			−133 (114)	166 (18)
PhC2			−114 (75)	110 (63)		149 (44)			−54 (39)	165 (69)
PhA			68 (48)	136 (51)		159 (37)			−125 (99)	162 (23)

Angle values averaged over the final 0.5 ns, i.e., last 1000 coordinate frames, are given with standard deviations in parenthesis. All values are in degrees. Dihedral angles of proline side chains are omitted.
[a] Coordinates of the x-ray structure [3].

Table 2. Backbone dihedral angles of antamanide

	Val1	Pro2	Pro3	Ala4	Phe5	Phe6	Pro7	Pro8	Phe9	Phe10
ϕ										
x-ray[a]	−113	−64	−79	−103	70	−78	−62	−92	−101	56
40 NOEs[b]	−114	−58	−89	−90	−87	−122	−74	−91	−81	−83
MEDUSA[c]	−7	−92	−95	−108	80	−96	−94	−95	−110	94
AnC	−94 (13)	−59 (8)	−75 (9)	−82 (12)	−81 (11)	−101 (22)	−64 (8)	−90 (11)	−74 (12)	58 (9)
AnA	−86 (15)	−64 (8)	−89 (11)	−71 (12)	59 (9)	−93 (19)	−63 (8)	−92 (11)	−71 (11)	58 (9)
ψ										
x-ray[a]	158	161	−20	−22	29	161	160	−4	−22	48
40 NOEs[b]	118	133	3	88	96	150	129	−1	81	78
MEDUSA[c]	104	151	55	−51	44	127	153	55	−56	−24
AnC	136 (11)	148 (9)	−56 (17)	119 (14)	98 (19)	137 (10)	141 (9)	−5 (22)	−42 (14)	48 (17)
AnA	130 (7)	141 (8)	−7 (17)	−42 (12)	61 (20)	136 (10)	138 (9)	−2 (20)	−43 (12)	52 (16)

Angle values averaged over the final 0.5 ns, i.e., last 1000 coordinate frames, are given with standard deviations in parenthesis. All values are in degrees.
[a] Coordinates of the x-ray structure [3].
[b] Coordinates from a 33 ps molecular dynamics simulation of antamanide which used 40 negative nuclear Overhauser enhancement (NOE) values as constraints [6]. The NOE values were measured at 500 MHz and 253 K.
[c] Conformation obtained from structure refinement using the multiconformational search protocol MEDUSA [20].

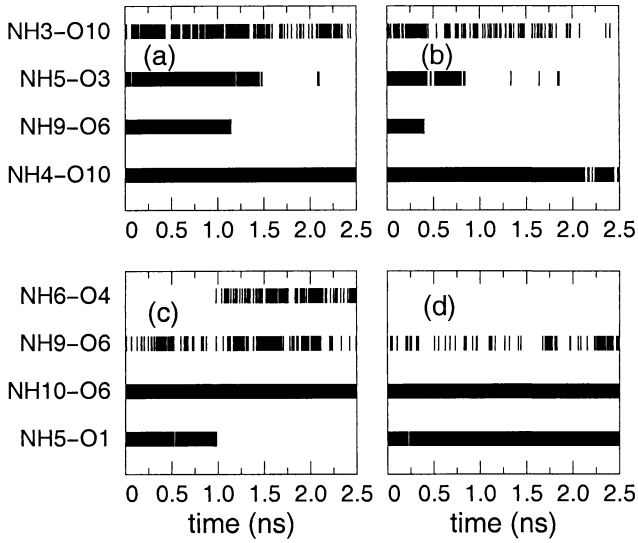

Figure 4. Evolution of the main-chain hydrogen bonds along the trajectory: (a) PhC1; (b) PhA; (c) AnC; (d) AnA. A hydrogen bond was considered formed if the donor-to-acceptor distance was less than 3.5 Å and the donor–hydrogen–acceptor angle was larger than 120°.

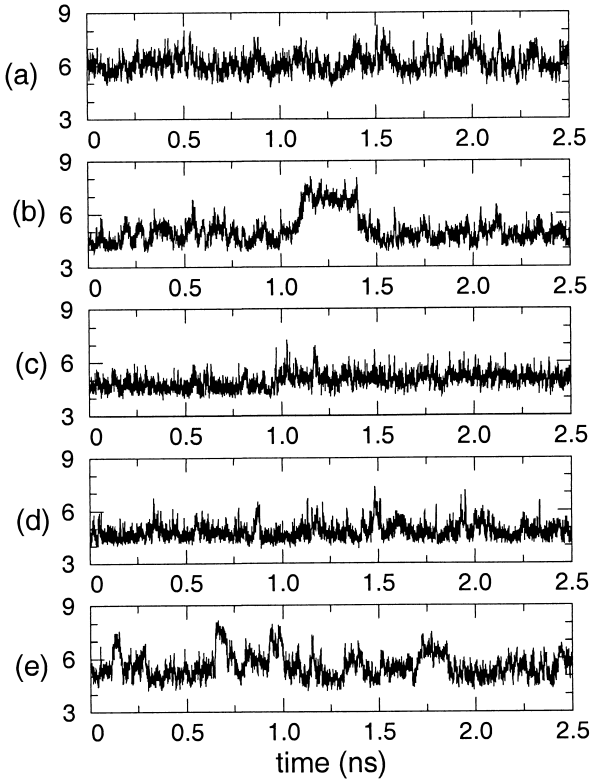

Figure 5. Aromatic–proline stacking in phakellistatin and antamanide. Intercentroid distances in Ångstroms between the rings of (a) Pro1 and Phe4 in the PhC1 run, (b) Pro7 and Tyr9 in PhC1, (c) Pro2 and Phe5 in AnC, (d) Pro7 and Phe10 in AnC, (e) and Pro8 and Phe9 in AnC.

bonds (19 ± 2 and 18 ± 2). In all simulations of antamanide there is a water molecule accepting from the main-chain amide of Val1 and Phe6, in agreement with the crystal structure[3] and the NMR relaxation measurements.[11]

3.4. Side–chain packing

In the crystal structure of phakellistatin the side chains of Pro1 and Phe4, and those of Pro7 and Tyr9, are stacked in a face-to-face arrangement.[2] Similar stacking of aromatic and pyrrolidine rings was found in the crystal structure of antamanide.[3] Moreover, an NMR solution structure of the linear peptide SYPFDV[21] and of molecular dynamics simulations[22,23] have shown that aromatic–proline interactions play an important role in the stabilization of secondary structure in short peptides.

For both cyclic peptides the time evolution of distances between aromatic and proline residues is plotted in Figure 5. The aromatic–pyrrolidine stacking is more stable in the antamanide trajectories than in the phakellistatin runs (see also below). Interestingly, the conformational transition from the saddle-like crystal structure of phakellistatin to a more elongated conformation (see Section 3.1) is coupled to the transient dissociation of the Pro7–Tyr9 side-chain pair at about 1.2 ns of PhC1 (Figure 5b), 0.2 ns of PhC2, and 0.4 ns of PhA. Hence, the transient separation of the Pro7–Tyr9 pyrrolidine–aromatic stacking is concomitant and might even trigger the conformational transition.

The relatively large number of transitions between stacked (S) and dissociated conformations (D) during the total simulation time of 7.5 ns for phakellistatin and 5 ns for antamanide allows an estimation of the free energy of stacking to be made. According to the Boltzmann statistics one can write

$$N_S/N_D = e^{-(G_S - G_D)/RT} \quad (1)$$

where N_S and N_D are the number of stacked and dissociated conformations, R is the gas constant, T is the temperature, and $G_S - G_D$ is the free energy of association of an aromatic–pyrrolidine side chain pair in water. Such a pair is considered stacked if the intercentroid distance is smaller than the average intercentroid distance along the trajectories, and dissociated if this distance is larger than the average distance augmented by a gap of 0.5 Å, which is the average deviation for the five runs. This yields a free energy of stacking of −0.6 and −0.7 kcal/mol for the phakellistatin Pro1–Phe4 and Pro7–Tyr9 pairs, respectively. The values for antamanide are −0.8, −1.0, and −0.6 kcal/mol for the pairs Pro2–Phe5, Pro7–Phe10, and Pro8–Phe9, respectively. There are no experimental data for a direct comparison. Yet, one can mention a double mutant cycle of barnase in which the stacking of the unprotonated imidazole of His18 and the indole of Trp94 was found to be favored by −0.4 kcal/mol relative to solvation by water.[24] The more favorable values obtained in this study might be due to the different residue types or the smaller entropy penalty because of the macrocyclic rigidity, or they might be a consequence of the approximations inherent to the force field.

3.5. Proline ring puckering

The puckering of the antamanide proline rings has been analyzed by molecular dynamics simulations with two different force fields[8,9] and compared with NMR data.[5] It was shown

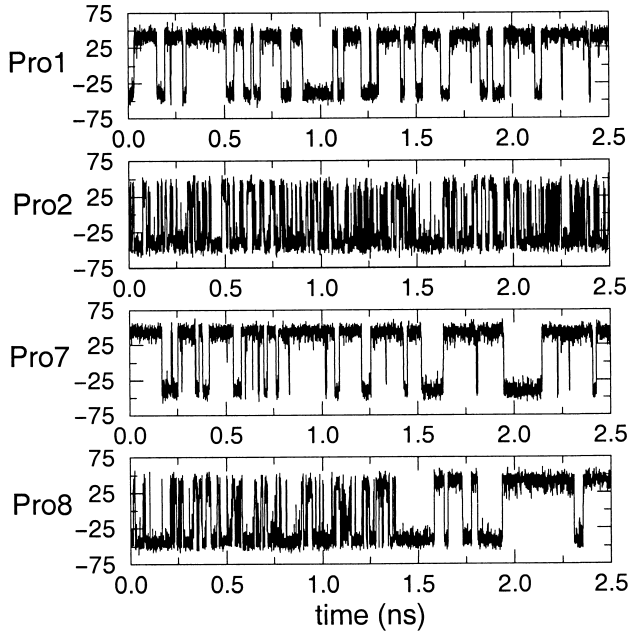

Figure 6. Proline χ_2 dihedral angle time series for the four proline residues from the PhC1 simulation of phakellistatin. Samples are plotted in increments of 0.5 ps.

that the dihedral angles of the side chains of Pro2, Pro3, and Pro7 exhibit fluctuations on a time scale of a few tens of picoseconds, which is much faster than for the backbone torsional mode. In the present work, individual time series for the dihedral angles were computed from all trajectories. The dihedral angle χ_2 varies the most during interconversion, together with χ_3. Hence, proline ring conformations are distinguished by the sign of χ_2 and will henceforth be referred as state *p* ($\chi_2 > 0$) and state *n* ($\chi_2 < 0$). The population of pucker state *p* for the AnC and AnA simulations is 73% (Pro2), 62% (Pro7), 43% (Pro3), and 33% (Pro8). This is in qualitative agreement with the population measured experimentally in solution: 65% (Pro2), 55% (Pro7), 10% (Pro3), and 0% (Pro8).[5]

For the phakellistatin run PhC1 the time series of the dihedral angle χ_2 of the four proline side chains is plotted in Figure 6. Similar behavior is found in the PhC2 and PhA simulations; the population of pucker state *p* for the three phakellistatin runs is 76% (Pro1), 35% (Pro2), 76% (Pro7), and 51% (Pro8). The proline pair 1–2 of phakellistatin and the proline pair 2–3 in antamanide have similar values for the total occupancy of each of the two pucker states. This might originate from the similarity in the phakellistatin α turn Ile10–Pro1–Pro2–Ile3–Phe4 (NH4–O10 hydrogen bond) and the antamanide α turn Val1–Pro2–Pro3–Ala4–Phe5 (NH5–O1 hydrogen bond).

The PhC1 time series of Pro8 shows a mixed behavior; it is predominantly in state *n* in the first half of the simulation while there is a significant occupancy of both states (and for large period of times up to about 0.25 ns) in the second half, i.e., after the backbone conformational transition described above. The change in behavior upon transition also takes place in PhC2 and PhA. This is consistent with the correlation of backbone conformation and proline ring mobility that was found experimentally[25] and by computational studies.[9]

3.6. Simulated conformation of phakellistatin in water

The C_α and heavy atom RMSDs from the phakellistatin conformation at the end of the PhC1 run were calculated for the 1 000 snapshots saved during the final 0.5 ns. The average values of the C_α RMSD for the PhC1, PhC2, and PhA trajectory are 0.5, 0.6, and 0.7 Å, respectively. The corresponding values for the heavy atom RMSD are 1.0, 1.2, and 1.5 Å. Therefore, the final snapshot of the PhC1 simulation (Figure 7) is a good representative of the predicted solution structure. It contains a ring inclusion water molecule that is hydrogen bonded to the NH groups of Val5 and Ile10, and the carbonyl oxygen of Leu6. In the crystal structure there is a water molecule that has a role similar to that of a transannular bridge but is involved in only two hydrogen bonds with the NH of Ile10 and the CO of Leu6.[2] In all phakellistatin runs the transition from the saddle-like crystal structure to the more elongated solution conformation is coupled with the formation of the additional hydrogen bond between the ring inclusion water molecule and the NH of Val5 and the concomitant rupture of the NH5–O3 hydrogen bond. The water molecule involved in three hydrogen bonds with phakellistatin has a residence time longer than 1 ns.

Table 1 shows the dihedral angle values averaged over the final 0.5 ns for the phakellistatin runs. The main differences from the backbone X-ray structure are localized in the ϕ and ψ angles of Tyr9 and the ψ angle of Phe4, Val5, and Pro8. The largest side-chain fluctuations involve the χ_2 angles of Phe4 and Tyr9. The motion of the latter is also shown with a trace rendering in Figure 7. There are conformational fluctuations on a time scale of less than 10 ps from a structure with the pyrrolidine–aromatic stacking, i.e., with face-to-face arrangement of the Pro1–Phe4 and Pro7–Tyr9 side chains and distant Phe4 and Tyr9 aromatic rings (thin lines in Figure 7), to a conformation with up to three edge-to-face interactions with significant van der Waals contacts between the Phe4 and Tyr9 side chains (thick lines in Figure 7). These side chains often assume a face-to-face conformation, with one aromatic ring shifted toward the C_β atom of the other aromatic side chain. Such dynamic behavior of the two aromatic rings is common to the three phakellistatin runs.

There is an analogous, although less pronounced, motion involving the Phe5 and Phe10 side chains of antamanide, which fluctuate between the face-to-face arrangement with the pyrrolidine rings of Pro2 and Pro7 and a conformation with close contacts between the Phe5 and Phe10 side chains and almost edge-to-face interactions between aromatic and pyrrolidine rings. The results of the simulations in aqueous solutions indicate that phakellistatin is more flexible than antamanide on a nanosecond time scale.

4. DISCUSSION

Three molecular dynamics simulations of phakellistatin in aqueous solution were initiated from the X-ray structure with different initial velocities and restraining conditions to prevent the decapeptide from leaving the center of the solvent sphere. The simulations yielded the same conformation, which is suggested to be a highly populated structure of phakellistatin in water. It is more elongated than the saddle-like crystal structure mainly because of the transition of the Tyr9 main-chain dihe-

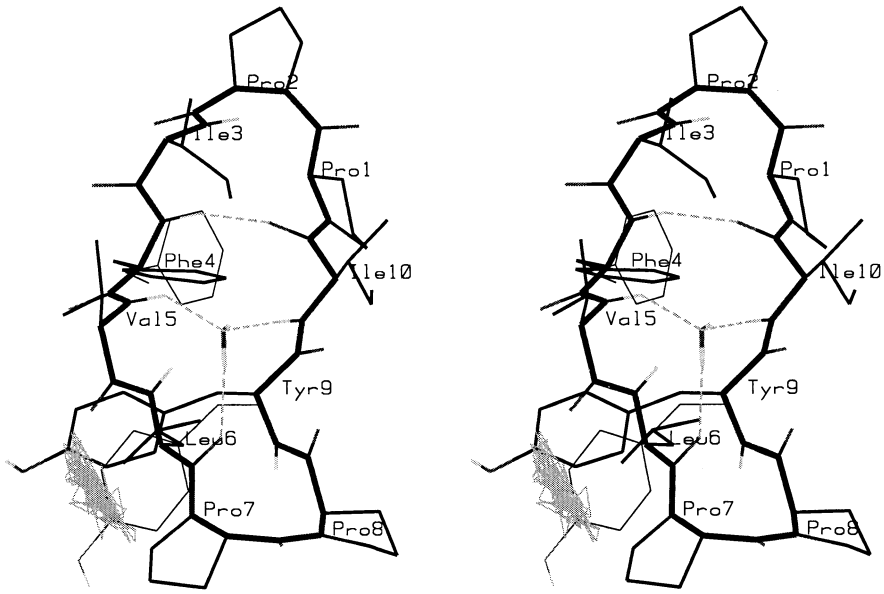

Figure 7. The phakellistatin structure at the end of the PhC1 run (thick lines for backbone and medium lines for side chains) is shown along with the conformation of the Phe4 and Tyr9 residues after 1.515 ns of PhC1 (thin lines). The trace of the C_ζ atom of Tyr9 is plotted in gray for snapshots taken every 5 ps from the final 1 ns of the PhC1 run. Also shown is the water molecule bridging the macrocycle. The water–phakellistatin and α-turn hydrogen bonds are drawn with dashed lines.

dral angles from the α_L to an extended region of the Ramachandran plot. This conformational change took place in all three phakellistatin simulations. It was coupled to the loss of the β-turn hydrogen bond, the transient dissociation of the Pro7–Tyr9 side-chain packing, and the formation of a third hydrogen bond between the NH group of Val5 and the water molecule acting as a transannular bridge in the crystal structure. This water molecule may be important for the stability of the elongated conformation.

As a basis of comparison the crystal structure of antamanide did not undergo significant changes in two molecular dynamics simulations that used the same conditions as for phakellistatin. This is in agreement with NMR data on an antamanide–$(H_2O)_n$ complex ($n \leq 2$).[11] In one of the two antamanide simulations a transition occurred in the Ala4–Phe5 peptide unit, which is consistent with structural data derived from NMR measurements in chloroform solution.[6] This is not a complete proof of the accuracy of the force field and the adequacy of the simulation protocol but allows to interpret the results of the phakellistatin simulations with more confidence. The calculated solution conformation of the two cyclic decapeptides are similar, particularly in their α-turn region, i.e., phakellistatin residues Ile10–Pro1–Pro2–Ile3–Phe4 and antamanide residues Val1–Pro2–Pro3–Ala4–Phe5. The pyrrolidine–aromatic stacking was more stable in antamanide than in phakellistatin. In the latter, the fluctuations in the side chains of Phe4 and Tyr9 may be important for conformational transitions connected with the binding of cations. It has been proposed that the formation of phakellistatin–metal complexes is implicated in the cancer cell growth-inhibitory properties of phakellistatin.[2]

Although the nanosecond time scale of the simulations is short for the sampling of all possible backbone transitions, the results of this computational study suggest a structure of phakellistatin that is likely to be significantly populated in aqueous solution. Testing of this prediction is a challenge for experimentalists.

ACKNOWLEDGMENTS

We thank Yu. V. Mitin and A.V. Finkelstein for interesting discussions and comments on the manuscript. We also thank N. Budin, P. Ferrara, and M. Scarsi for helpful discussions. Figures 2 and 7 were prepared with the molecular modeling program WITNOTP, kindly provided by Armin Widmer (Novartis Pharma AG, Basel, Switzerland).

This work was supported by the Cancer League of the Canton Zürich, the Swiss National Science Foundation (Nationalfonds, Grant 31-53604.98), and the Russian Basic Research Foundation (Grant 98-04-49303).

REFERENCES

1. Pettit, G.R., Xu, J., Dorsaz, A., Williams, M.D., Boyd, M.R., and Cerny, R.L. Isolation and structure of the human cancer cell growth inhibitory cyclic decapeptides phakellistatins 7, 8 and 9. *Biorg. Med. Chem. Lett.* 1995, **5,** 1339–1344
2. Herald, D.L., Cascarano, G.L., Pettit, G.R., and Srirangam, J.K. Crystal conformation of the cyclic decapeptide phakellistatin 8: Comparison with antamanide. *J. Am. Chem. Soc.* 1997, **119,** 6962–6973
3. Karle, I.L., Wieland, T., Schermer, D., and Ottenheym, H.C.J. Conformation of uncomplexed natural antamanide crystallized from CH_3CN/H_2O. *Proc. Natl. Acad. Sci. U.S.A.* 1979, **76,** 1532–1536

4. Kessler, H., Müller, A., and Pook, K. Assignment of all proton, carbon, and nitrogen NMR signals of antamanide in chloroform solution. *Liebigs Ann. Chem.* 1989, 903–912
5. Mádi, Z.L., Griesinger, C., and Ernst, R.R. Conformational dynamics of proline residues in antamanide. *j* coupling analysis of strongly coupled spin systems based on E. COSY spectra. *J. Am. Chem. Soc.* 1990, **112,** 2908–2914
6. Kessler, H., Bats, J.W., Lautz, J., and Müller, A. Conformation of antamanide. *Liebigs Ann. Chem.* 1989, 913–928
7. Brüschweiler, R., Roux, B., Blackledge, M., Griesinger, C., Karplus, M., and Ernst, R.R. Influence of rapid intramolecular motion on NMR cross-relaxation rates. A molecular dynamics study of antamanide in solution. *J. Am. Chem. Soc.* 1992, **114,** 2289–2302
8. Brunne, R.M., van Gunsteren, W.F., Brüschweiler, R., and Ernst, R.R. Molecular dynamics simulation of the proline conformational equilibrium and dynamics in antamanide using the GROMOS force field. *J. Am. Chem. Soc.* 1993, **115,** 4764–4768
9. Schmidt, J.M., Brüschweiler, R., Ernst, R.R., Dunbrack, R.L., Joseph, D., and Karplus, M. Molecular dynamics simulation of the proline conformational equilibrium and dynamics in antamanide using the CHARMM force field. *J. Am. Chem. Soc.* 1993, **115,** 8747–8756
10. Bremi, T., Brüschweiler, R., and Ernst, R.R. A protocol for the interpretation of the side-chain dynamics based on NMR relaxation: Application to phenylalanines in antamanide. *J. Am. Chem. Soc.* 1997, **119,** 4272–4284
11. Peng, J.W., Schiffer, C.A., Xu, P., van Gunsteren, W.F., and Ernst, R.R. Investigations of peptide hydration using NMR and molecular dynamics simulations: A study of effects of water on the conformation and dynamics of antamanide. *J. Biomol. NMR* 1996, **8,** 453–476
12. Brooks, B.R., Bruccoleri, R.E., Olafson, B.D., States, D.J., Swaminathan, S., and Karplus, M. CHARMM: A program for macromolecular energy, minimization, and dynamics calculations. *J. Comput. Chem.* 1983, **4,** 187–217
13. Neria, E., Fischer, S., and Karplus, M. Simulation of activation free energies in molecular systems. *J. Chem. Phys.* 1996, **105,** 1902–1921
14. Jorgensen, W.L., Chandrasekhar, J., Madura, J., Impey, R.W., and Klein, M.L. Comparison of simple potential functions for simulating liquid water. *J. Chem. Phys.* 1983, **79,** 926–935
15. Brünger, A. and Karplus, M. Polar hydrogen positions in proteins: Empirical energy placement and neutron diffraction comparison. *Proteins Struct. Funct. Genet.* 1988, **4,** 148–156
16. Beglov, D. and Roux, B. Finite representation of an infinite bulk system: Solvent boundary potential for computer simulations. *J. Chem. Phys.* 1994, **100,** 9050–9063
17. Brooks, C.L., III and Karplus, M. Solvent effects on protein motion and protein effects on solvent motion. *J. Mol. Biol.* 1989, **208,** 159–181
18. Ryckaert, J.P., Ciccotti, G., and Berendsen, H.J.C. Numerical integration of the Cartesian equation of motion of a system with constraints: Molecular dynamics of *n*-alkanes. *J. Comput. Phys.* 1977, **23,** 327–341
19. Pettit, G.R., Srirangam, J.K., Herald, D.L., Xu, J.P., Boyd, M.R., Cichacz, Z., Kamano, Y., Schmidt, J.M., and Erickson, K.L. Isolation and crystal structure of stylopeptide 1, a new marine *Porifera* cycloheptapeptide. *J. Org. Chem.* 1995, **60,** 8257–8261
20. Brüschweiler, R., Blackledge, M., and Ernst, R.R. Influence of rapid intramolecular motion on NMR cross-relaxation rates. A molecular dynamics study of antamanide in solution. *J. Biomol. NMR* 1991, **1,** 3–11
21. Yao, J., Dyson, H.J., and Wright, P.E. Three-dimensional structure of a type VI turn in a linear peptide in water solution. Evidence for stacking of aromatic rings as a major stabilizing factor. *J. Mol. Biol.* 1994, **243,** 754–766
22. Demchuk, E., Bashford, D., and Case, D.A. Dynamics of a type VI reverse turn in a linear peptide in aqueous solution. *Folding Design* 1997, **2,** 35–46
23. Mohanty, D., Elber, R., Thirumalai, D., Beglov, D., and Roux, B. Kinetics of peptide folding: Computer simulations of SYPFDV and peptide variants in water. *J. Mol. Biol.* 1997, **272,** 423–442
24. Loewenthal, R., Sancho, J., and Fersht, A.R. Histidine–aromatic interactions in barnase. *J. Mol. Biol.* 1992, **224,** 759–770
25. Cung, M.T., Vitoux, B., and Marraud, M. Flexibility of Pro–Pro sequences: IR and NMR experiments. *New. J. Chem.* 1987, **11,** 503–510